Supplementary Information

Apigenin is a direct small-molecule inhibitor of LAG-3 that synergizes with PD-L1 blockade for cancer immunotherapy

Konrad Barnowski [a,b], Marzena Lenart [c], Ping Lv [d], Sylwia Wójcik a,b, Katarzyna Nakielska [a,c], Justyna Kocik-Król [a], Judyta Cielecka-Piontek[g], Anna Stasiłowicz-Krzemień[g], Fusco Riccardo [e], Alexander Doemling [e], Justyna Kalinowska-Tłuścik [a], Marta Karpiel [a,b], Szymon Buda [a], Katarzyna Magiera-Mularz [a], Ewa Surmiak [a], Bogdan Musielak [a], Maciej Siedlar [c], Bozena Skupien-Rabian [f,h], Urszula Jankowska f, Wen Zhang* [d], Jacek Plewka* [a]

[a]Faculty of Chemistry, Jagiellonian University, Gronostajowa 2, 30-387 Krakow, Poland;

[b]Jagiellonian University, Doctoral School of Exact and Natural Sciences, prof. St. Łojasiewicza 11, 30-348 Krakow, Poland

[c]Department of Clinical Immunology, Institute of Pediatrics, Jagiellonian University Medical College, Wielicka 265, 30-663 Krakow, Poland

[d]Lab of Chemical Biology and Molecular Drug Design, College of Pharmaceutical Science, Zhejiang University of Technology, Deqing 313299, China

[e]Czech Advanced Technology and Research Institute (CATRIN), Palacký University Olomouc, Šlechtitelů 27, 77900 Olomouc, Czech Republic

[f] Proteomics Core Facility, Malopolska Centre of Biotechnology, Jagiellonian University, Krakow, Poland

[g]Department of Pharmacognosy and Biomaterials, Poznan University of Medical Sciences, Rokietnicka 3, 60-806 Poznan, Poland

[h]Proteomics Core Facility, Faculty of Biochemistry, Biophysics and Biotechnology, Jagiellonian University, Krakow, Poland

*Email: jacek.plewka@uj.edu.pl wzhang63@zjut.edu.cn

This document contains Supplementary Figures S1–S10.

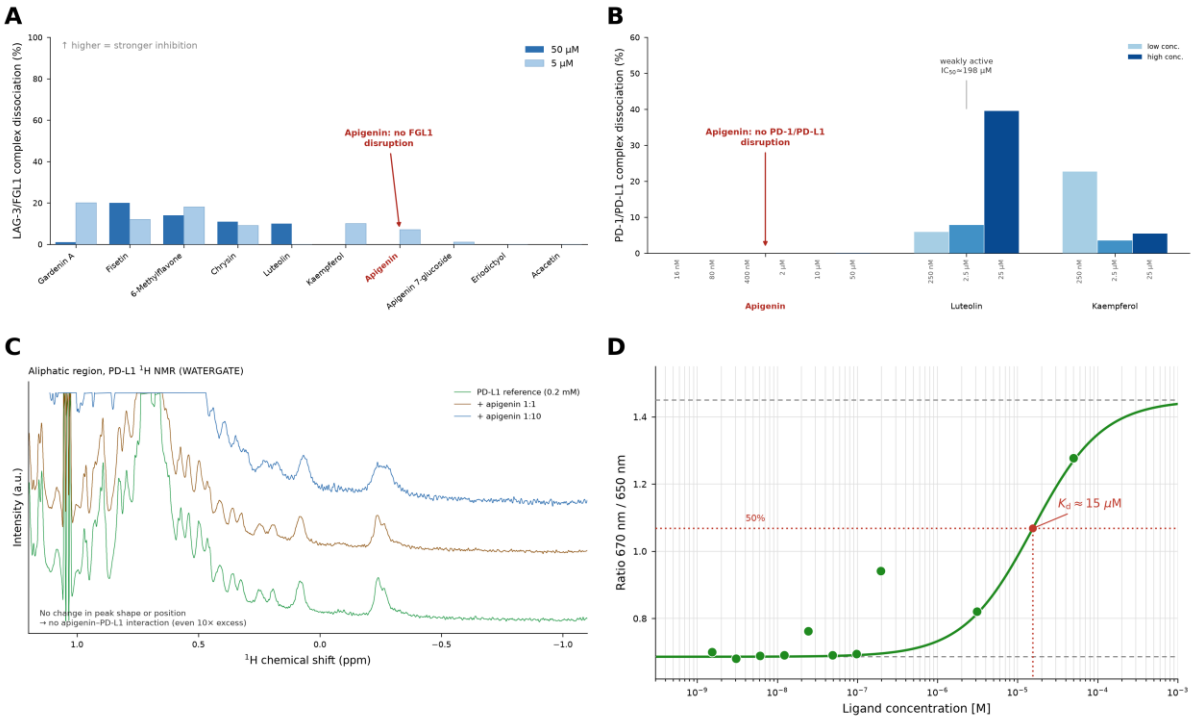

Figure S1. Apigenin selectively engages LAG-3 without disrupting the PD-1/PD-L1 axis or binding PD-L1. (A) LAG-3/FGL1 HTRF counter-screen at 50 and 5 µM; apigenin produced essentially no disruption (~0%), confirming it does not interfere with the LAG-3/FGL1 interaction. (B) PD-1/PD-L1 HTRF assay (Cis-Bio); apigenin and kaempferol were inactive and luteolin showed only weak activity (IC50 ≈ 198 µM), indicating the flavonoids do not target the PD-1/PD-L1 axis. (C) ^{1}H NMR WATERGATE spectra of the aliphatic region of PD-L1 (green, reference 0.2 mM in PBS; brown, 1:1; blue, 1:10 apigenin excess); no change in peak shape or position was observed, confirming the absence of direct apigenin–PD-L1 binding. (D) Microscale thermophoresis (spectral shift) of His-tagged LAG-3 with apigenin in 1% DMSO; the 670/650 nm ratio yields an apparent dissociation constant of Kd ≈ 15 µM determined by plateau-midpoint construction.

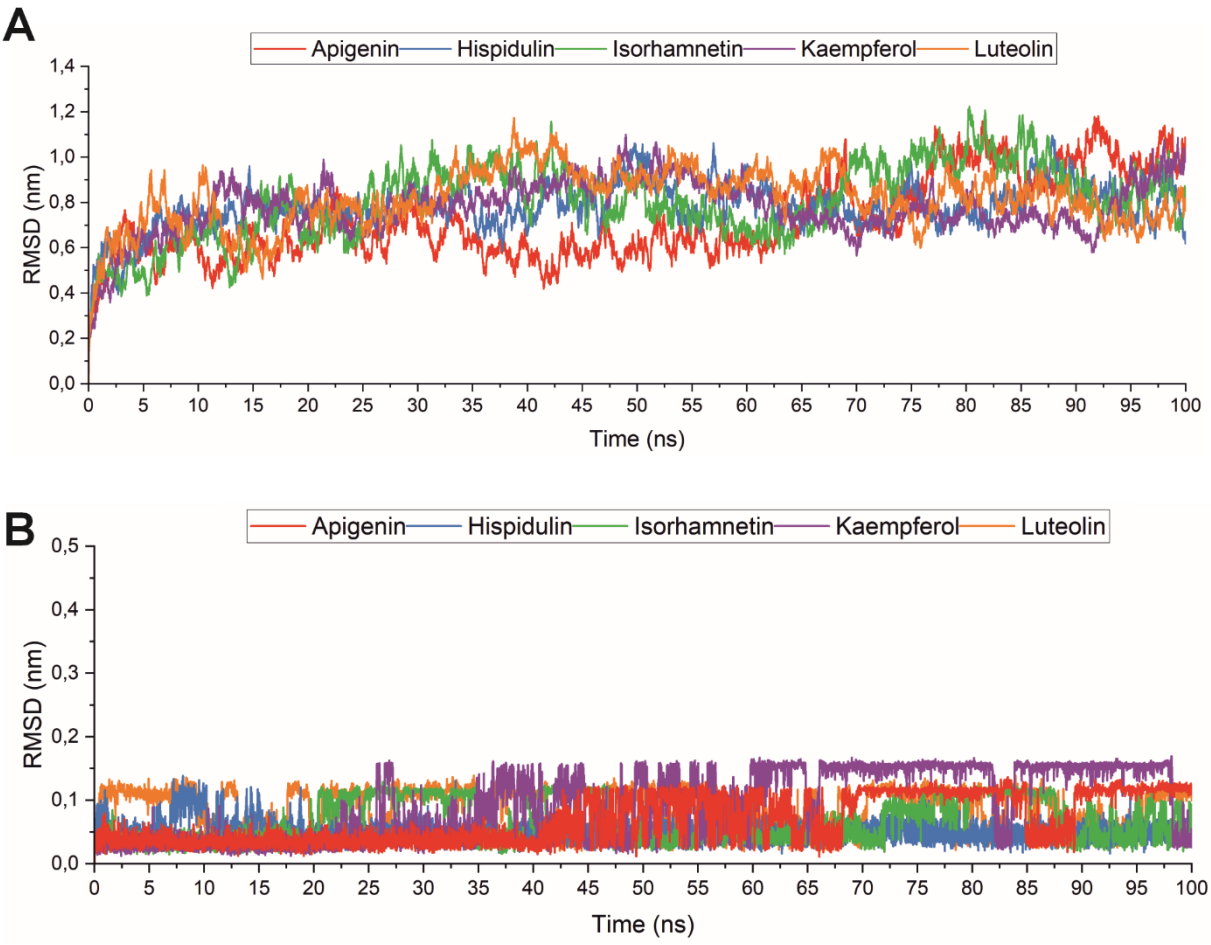

Figure S2. Molecular dynamics simulations confirm the stability of flavonoid–LAG-3 complexes. (A) Root-mean-square deviation (RMSD) of the LAG-3 protein backbone in complex with each of the five most potent flavonoids over 100 ns of simulation. (B) RMSD of the corresponding flavonoid ligands. All systems remained stable throughout the simulation time, with ligands retained within the predicted binding site located between the D1 and D2 domains.

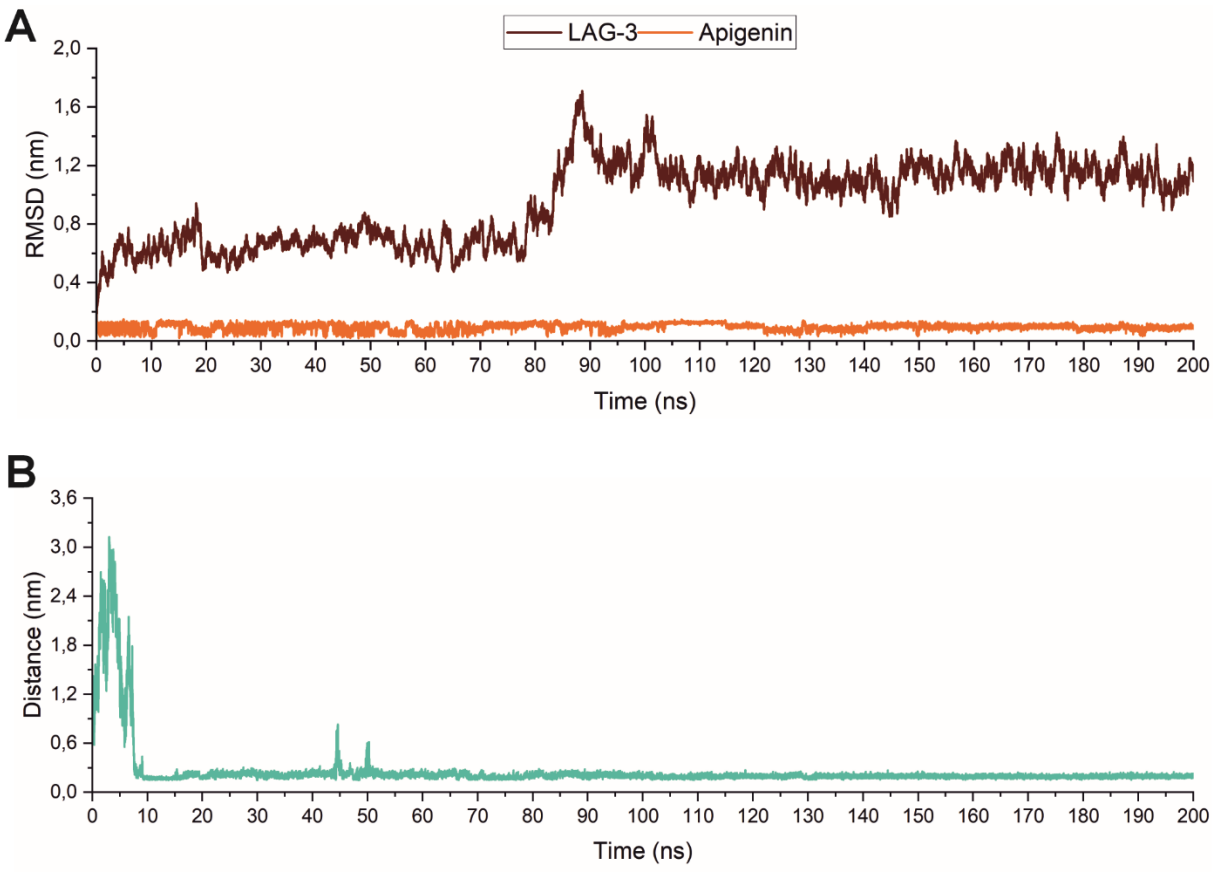

Figure S3. An extended 200 ns simulation independently confirms the apigenin binding site. (A) RMSD of the LAG-3 protein and of the apigenin molecule throughout a 200 ns simulation initiated from unbound apigenin, indicating high stability of the system. (B) Distance between LAG-3 and apigenin over the simulation time; after ~10 ns apigenin formed interactions in close proximity to the predicted binding site and, following a small rearrangement over the next ~60 ns, remained stably bound thereafter.

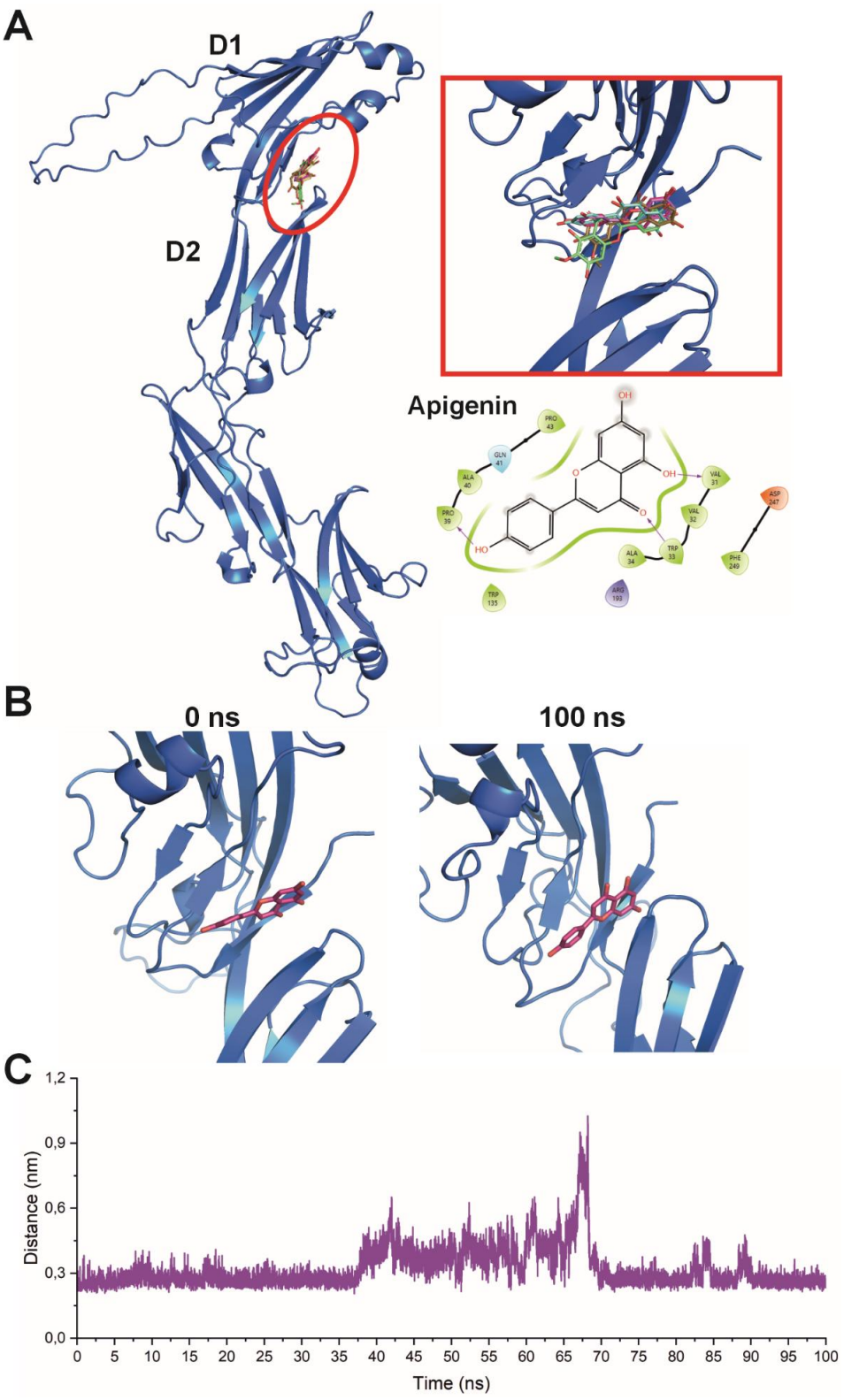

Figure S4. Docking and molecular-dynamics analysis of the apigenin–LAG-3 complex. (A) Two-dimensional protein–ligand interaction map for the LAG-3/apigenin docking pose. (B) First and final frames from the molecular-dynamics simulation of the LAG-3/apigenin complex, showing retention of the

ligand within the selected binding site. (C) Distance between the apigenin molecule and the LAG-3 binding-site center (Trp33 backbone oxygen atom) over the simulation.

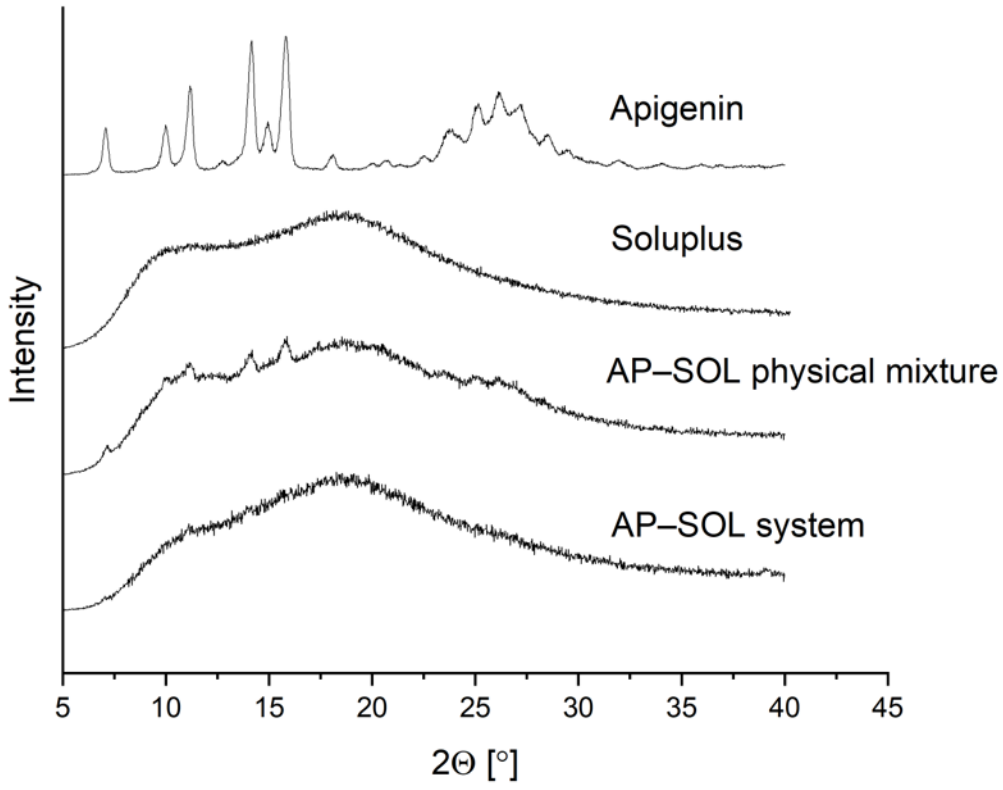

Figure S5. X-ray powder diffraction confirms conversion of apigenin into an amorphous solid dispersion. XRPD patterns of crystalline apigenin (Apigenin), the Soluplus carrier (Soluplus), their physical mixture (AP–SOL physical mixture), and the formulated apigenin solid dispersion (AP–SOL system). Crystalline apigenin displays sharp, characteristic Bragg reflections, which are retained in the physical mixture but are absent from the AP–SOL system, where only a broad amorphous halo remains. Loss of the crystalline peaks confirms amorphization of apigenin within the formulation. These XRPD data have been reported previously in Stasiłowicz-Krzemień et al. (Int. J. Mol. Sci. 2025, 26, 8126; https://doi.org/10.3390/ijms26178126) and are reproduced here under the terms of the Creative Commons CC BY 4.0 license.

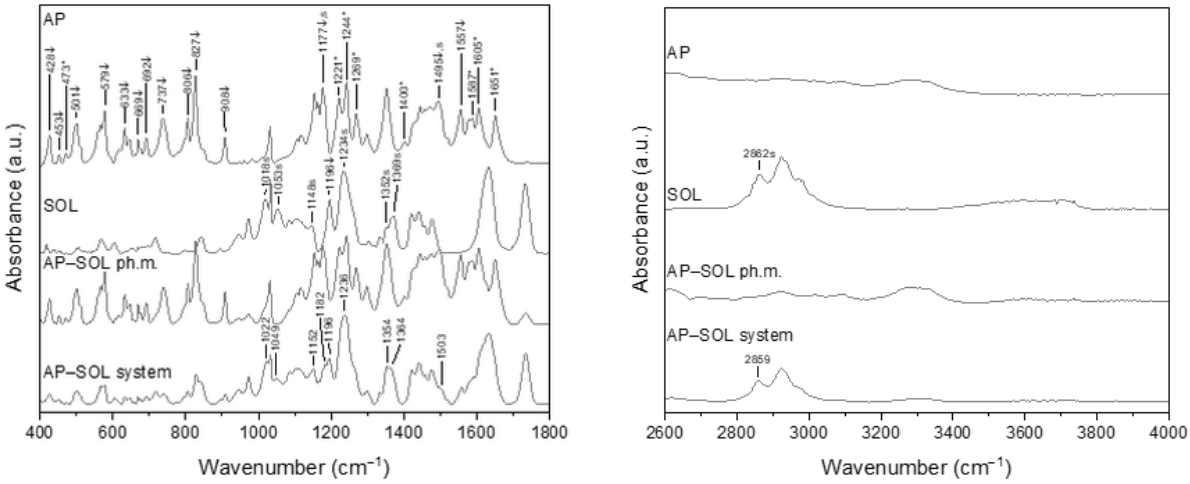

Figure S6. FTIR spectra are consistent with dispersion of apigenin in the Soluplus matrix. Fourier-transform infrared spectra of apigenin (AP), Soluplus (SOL), their physical mixture (AP–SOL ph.m.), and the formulated solid dispersion (AP-SOL system), shown for the fingerprint region (400–1800 cm^{-1}, left) and the C–H/O–H stretch region (2600–4000 cm^{-1}, right). The sharp apigenin bands present in AP and the physical mixture are broadened and attenuated in the AP–SOL system, consistent with the loss of crystalline order and molecular dispersion of apigenin within the polymer matrix. These FTIR data have been reported previously in Stasiłowicz-Krzemień et al. (Int. J. Mol. Sci. 2025, 26, 8126; https://doi.org/10.3390/ijms26178126) and are reproduced here under the terms of the Creative Commons CC BY 4.0 license.

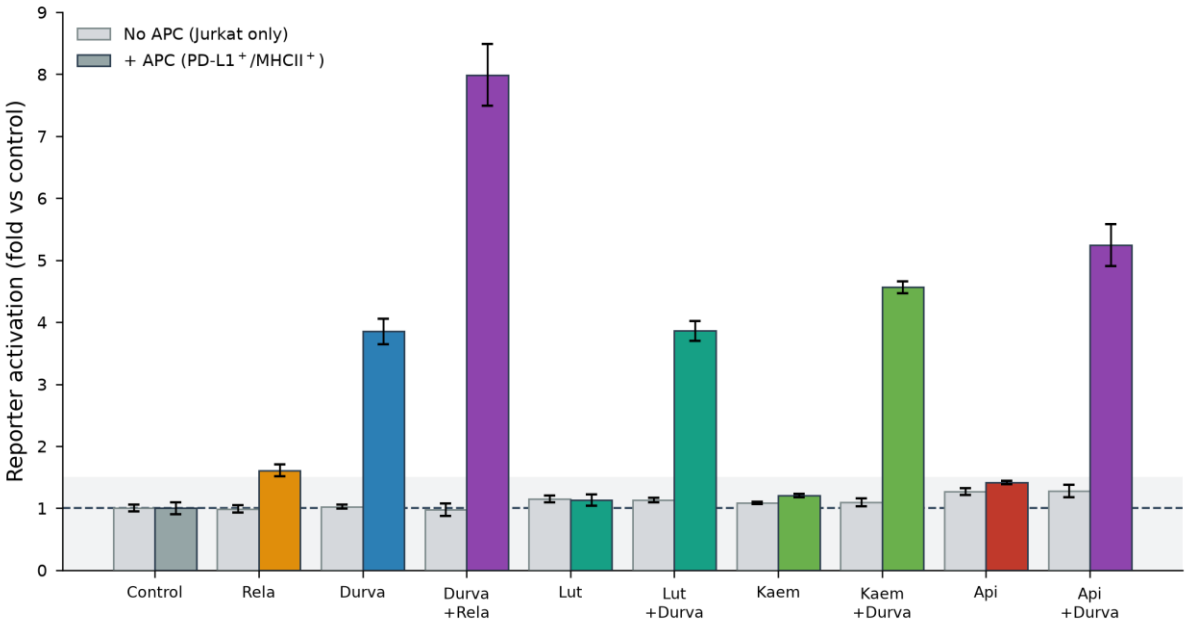

Figure S7. Reporter activation is strictly antigen-presenting-cell dependent. NFAT-luciferase Jurkat reporter effector cells were treated with the indicated agents either alone (no APC; grey bars) or co-cultured with PD-L1^{+}/MHCII^{+} antigen-presenting cells (+ APC; colored bars). Bars are luminescence normalized to untreated control (mean ± SD). In the absence of APCs, no treatment - durvalumab, relatlimab, the durvalumab/relatlimab combination, or any flavonoid (luteolin, kaempferol, apigenin) alone or with durvalumab - elevated reporter signal above the 0.97–1.28 baseline band. The identical treatments produced 4- to 8-fold activation only when APCs were present, confirming that reporter output reflects checkpoint engagement at the APC–effector synapse rather than a direct action of any compound on the effector reporter cell. Doses shown at 10 µM.

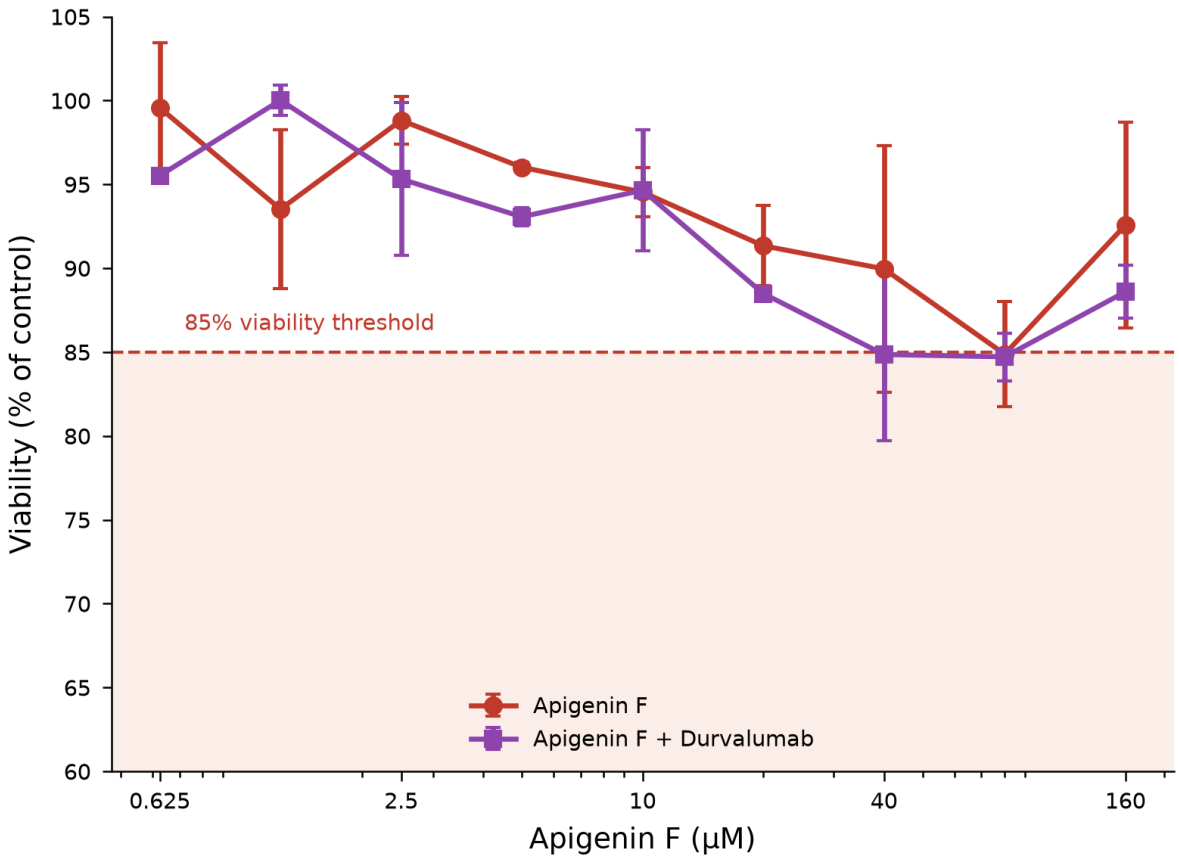

Figure S8. Formulated apigenin preserves cell viability across the dose range. Cell viability (percentage of untreated control) of the reporter co-culture treated with formulated apigenin (Apigenin F) or formulated apigenin plus durvalumab (Apigenin F + Durvalumab) across the 0.625–160 μM dose range (mean ± SD). Viability remained at or above 85% at all concentrations for both conditions (minimum ≈ 85% at 80 μM), confirming that the reporter activation observed at these doses is not confounded by cytotoxicity.

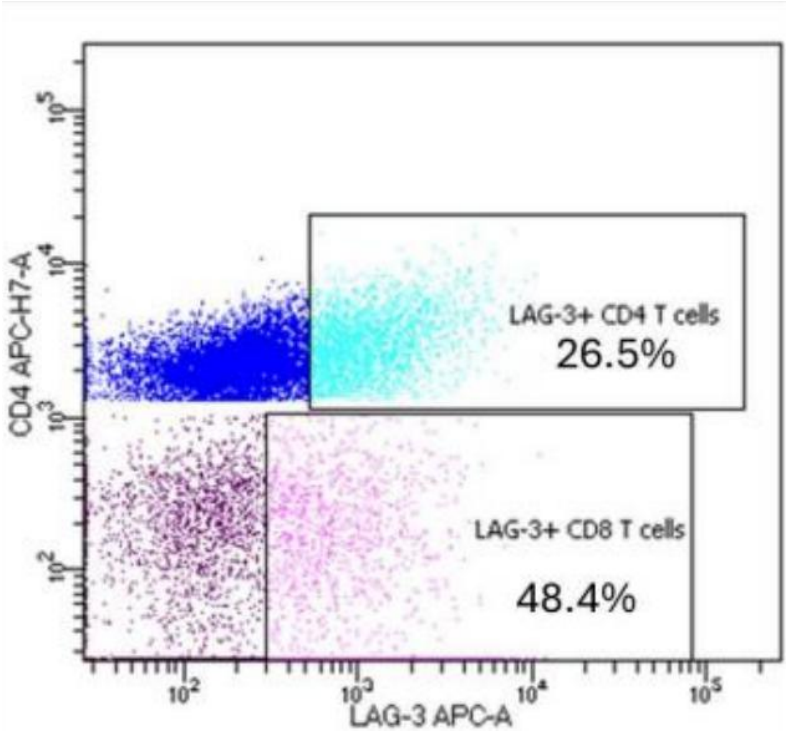

Figure S9. LAG-3 is upregulated on CD4$^+$ and CD8$^+$ T cells following stimulation. Flow-cytometric analysis of peripheral blood mononuclear cells (PBMC) from healthy-donor blood following stimulation, showing elevated LAG-3 expression on T cells. Cells were stained for CD4 (APC-H7) and LAG-3 (APC) and gated to quantify LAG-3-expressing populations. LAG-3$^+$ cells comprised 26.5% of CD4$^+$ T cells and 48.4% of CD8$^+$ T cells, confirming that the LAG-3 target is upregulated on both major T-cell subsets in primary human samples.

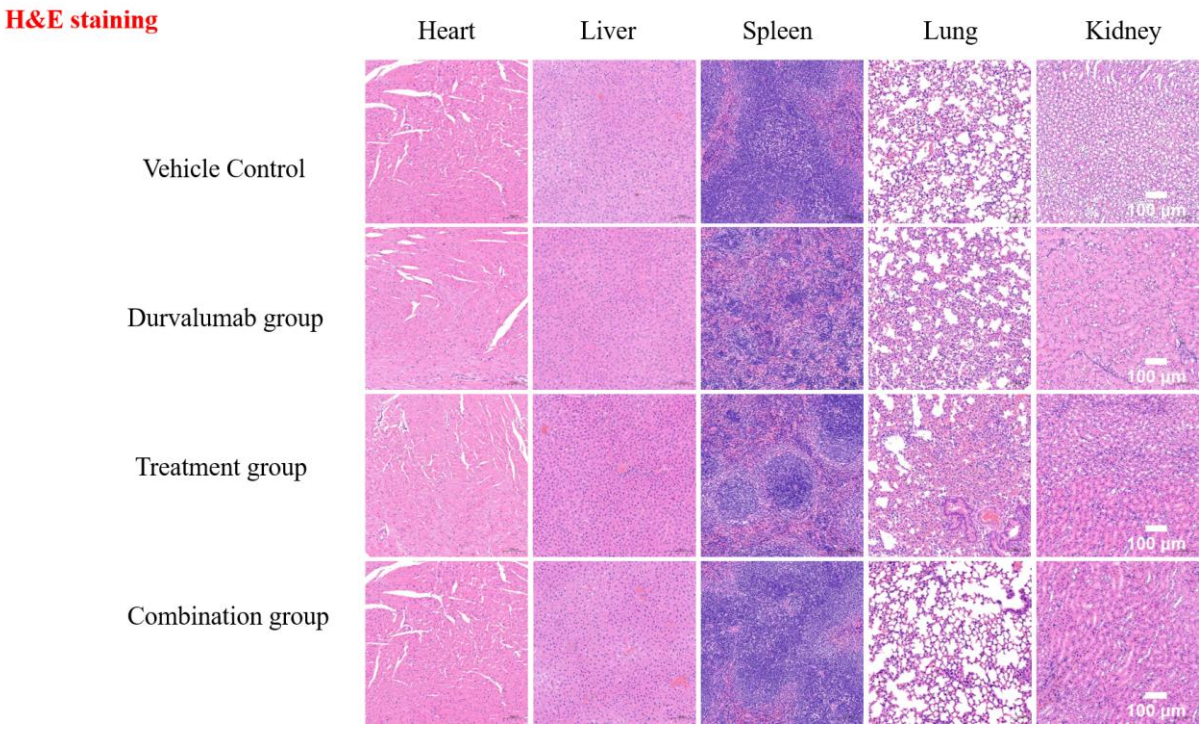

Figure S10. Apigenin, durvalumab, and their combination are well tolerated with no organ histopathology. Representative hematoxylin and eosin (H&E)-stained sections of heart, liver, spleen, lung, and kidney harvested at study endpoint from MC38 tumor-bearing mice treated with vehicle control, durvalumab, apigenin (treatment group), or the combination. No treatment-related histopathological abnormalities, necrosis, or inflammatory infiltrates were observed in any organ across the treatment groups, indicating that the combination regimen is well tolerated. Scale bar, 100 μm.